PHYSICAL REVIEW A **77**, 041601(R) (2008)

Optical control of the internal and external angular momentum of a Bose-Einstein condensate

K. C. Wright,[1] L. S. Leslie,[2] and N. P. Bigelow[1,2]
[1]*Department of Physics and Astronomy, University of Rochester, Rochester, New York 14627, USA*
[2]*Institute of Optics, University of Rochester, Rochester, New York 14627, USA*
(Received 13 December 2007; published 1 April 2008)

We present experimental results on the coherent transfer of orbital angular momentum (OAM) from optical fields to the center-of-mass motion of a Bose-Einstein condensate (BEC), using an approach which results in negligible linear momentum change. Two collinear optical beams of differing OAM are used to couple discrete sublevels of the atomic ground state via a stimulated Raman process. We demonstrate several of the possible optical field configurations which place the BEC into various spinor and vortex states. We also show how this approach can be used to create coherent superpositions of these states and use the interference patterns of such superpositions to confirm the presence of quantized vortices.

DOI: 10.1103/PhysRevA.77.041601 PACS number(s): 03.75.Lm, 37.10.Vz, 03.75.Mn, 37.25.+k

Recent developments in atomic physics and optics have clarified important parallels between the angular momentum degrees of freedom of both coherent light and matter. It has been long understood that photons possess a quantized internal spin corresponding to their polarization state, and that in atom-photon interactions this internal angular momentum can be coupled to the internal spin state of the atomic system. [1,2] More recently, it has been shown that optical fields also possess an external degree of freedom allowing them to carry quantized angular momentum in their spatial mode [3–5], which can couple to the external angular momentum (i.e., center-of mass motion) of an atom.

Orbital angular momentum (OAM) states of light, which include the Laguerre-Gaussian (LG) spatial modes, are characterized by azimuthal phase winding about singularities in the field [3]. In LG beams, the phase winding number (l) corresponds to a quantized amount of OAM ($l\hbar$) carried in the mode. These so-called "vortex states" of light have a direct counterpart in coherent matter systems such as superfluid helium [6,7] and Bose-condensed atomic gases (BEC) [8,9]. In such systems, external angular momentum appears as quantized vortices in the macroscopic many-body wave function of the system. The idea of coupling between optical vortex beams and BEC vortex states was first suggested a decade ago [10]. Significant theoretical work has been done [11–16] to refine the physical picture of this interaction, however, there has been little progress toward experimental implementation of such a vortex-coupling scheme until recently [17].

In the interim, a number of different techniques, such as the "phase engineering" approach [8,18], optical [19] and magnetic [20] stirring techniques, and optical [21] and magnetic topological phase imprinting [22] have been used to create vortices in BECs with well-documented success. The angular momentum transfer technique we demonstrate here is distinguished from each of these other methods by at least one of the following characteristics. First, the amount of angular momentum transferred is well-defined, being unambiguously determined by the angular momentum state of the optical fields used. Second, the transfer process can be performed repeatedly on comparatively short time scales (μs), allowing rapid creation and manipulation of coherent superpositions of vortex states. Third, the spin and vortex states created in the BEC can be as spatially complex as the optical beam modes used to create them, which could be generated, for example, by means of a spatial light modulator.

The two-photon interaction we have used to transfer angular momentum from optical fields to a BEC is illustrated schematically in Fig. 1. Three states are coupled by a pair of laser beams in a lambda configuration, such that atoms initially in one ground state sublevel are coherently transferred to another sublevel, without populating the excited state. Conservation of momentum dictates that the atoms must acquire the difference in the momentum of the two fields. The change in the atoms' internal spin state is determined by the polarizations of the two light fields. Similarly, the atoms' external spin state (center-of-mass motion around a chosen quantization axis) must change if there is a difference in the external angular momentum of the two optical fields. If the lasers are copropagating and the energy difference between the two atomic ground states is small compared to the photon energy, then the change in linear momentum is much smaller than the momentum uncertainty of the BEC and can be neglected. For example, $\Delta v_{\|}=\Delta E/mc \approx 50$ pm/s in our experiment.

The angular momentum transfer technique recently used by Andersen *et al.* [17] is an ingenious modification of this

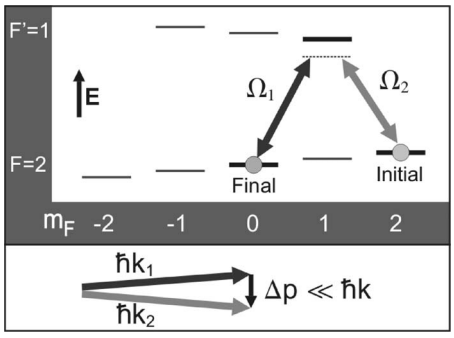

FIG. 1. Energy and momentum representation of the two-photon interaction used in the experiment. The atomic states shown are part of the ^{87}Rb $D1$ hyperfine structure. Atoms in the BEC, initially in the $|F=2,m_F=2\rangle$ state, are coupled into the $|F=2,m_F=0\rangle$ state by the application of the indicated laser fields Ω_1, Ω_2.

general idea, with several key differences between it and the internal-state method described in the literature and used in our work. The contrasting feature of that work was that counterpropagating laser pulses were used to couple *linear momentum* states of the BEC, rather than *internal* states. In such a configuration, the linear momentum change is necessarily much larger ($\approx 2\hbar k$) than the momentum uncertainty of the BEC, causing the components of the cloud to physically separate after the interaction. We stress that our method of adiabatic transfer between internal states avoids this issue, however, a very stable magnetic bias field is required to precisely control the internal state energies. The ability to change the internal spin state of the atom is an important feature in itself, allowing the preparation of complex spin textures of the BEC, with or without imparting OAM. In atomic systems with many ground state sublevels, such as ^{87}Rb, multiple components of the spinor wave function of the BEC can be controlled by sequential, pairwise coupling of selected sublevels with appropriate optical fields.

The multilevel nature of the alkali metal atoms introduces several potential complications that must be dealt with to ensure successful coherent population transfer between a selected pair of magnetic sublevels (see [23] and references therein). Adiabatic evolution of the system from an initial bare state to a desired final state requires the existence of a dressed state of null eigenvalue (dark state) connecting them that remains well separated from other dressed states as the system evolves. For the work described in this Rapid Communication, in which we couple the $F=2$, $m_F=2,0,-2$ states via the $F'=1$, $m_F=1,-1$ states (denoted $|2\rangle$, $|0\rangle$, $|-2\rangle$, $|1'\rangle$, and $|-1'\rangle$ hereafter), we have determined that limiting the Rabi frequencies to no more than half the Zeeman splitting of the ground state sublevels is sufficient to prevent problems due to dressed state level crossings. We apply a uniform magnetic bias field of 17 G, which is sufficient to separate the adjacent ground state sublevels by 12 MHz, or twice the natural linewidth. At this field value, the second-order Zeeman shift of the $|0\rangle$ state ($\approx$83 kHz) exceeds the two-photon linewidth (typically $<$40 kHz). This allows the two-photon transition from $|2\rangle$ to $|0\rangle$ to be addressed independently from the $|0\rangle$ to $|-2\rangle$ transition.

Our experimental procedure can be functionally divided into three stages: target preparation, interaction, and imaging. The preparation stage begins with the production of a BEC of 10^6 ^{87}Rb atoms, spin-polarized in the $|2\rangle$ state in a Ioffe-Pritchard magnetic trap. The trapping fields are then turned off and the BEC expands and falls for 9 ms, during which time the diameter of the cloud increases to 70 μm. After this expansion, the atomic density is low enough (5×10^{12} atoms/cm^3) that we have found it unnecessary to chirp the two-photon detuning during the optical interaction, as predicted in Ref. [10] for denser BECs. This delay also allows the strong magnetic trapping fields to decay and be replaced by the uniform 17 G axial bias field, which is calibrated and stabilized to better than 20 mG.

After the 9 ms target preparation stage, the Stokes and pump laser pulses (see Figs. 1 and 2) are sequentially applied to the BEC, with propagation axes aligned parallel to the magnetic bias field and the symmetry axis of the BEC. The spot sizes of these beams are typically 200 μm for a Gaussian spatial mode, or 70 μm for a LG mode. The LG modes are generated by passing a collimated Gaussian beam through a spiral phase plate which imparts a 2π azimuthal phase winding. The beam is allowed to propagate to the far-field and apodized. Field detunings are varied in a manner described in the results section. The pulses have a roughly Gaussian temporal profile with a duration of 60 μs. The temporal delay between the peak of the Stokes and pump pulses is set to 30 μs for on-resonant coherent population transfer, or 10 μs for off-resonant multipulse coherent transfer configurations. For multiple step sequences, the delay between operations is 10 μs. The on-resonant Rabi frequencies varied from 0.5–10 MHz, requiring peak beam powers of $<$100 μW. The two-photon detuning is fine-tuned to resonance by optimizing the population transfer at low beam intensity.

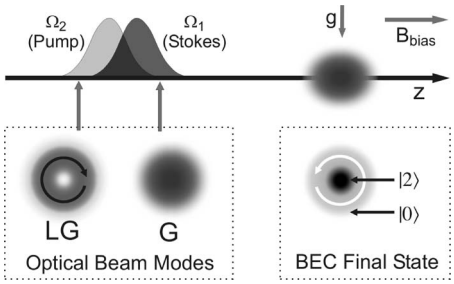

FIG. 2. Schematic of the experiment geometry showing the orientation of the optical pulses with respect to the BEC, magnetic field, and gravity. The boxed insets show axial views of one possible choice of optical beam modes and the resulting coreless vortex state of the BEC [e.g., Fig. 3(d)].

Once the pump and Stokes pulses have been applied, the BEC is in a mixed spin state, with different components physically overlapping (see Fig. 2 inset). In order to image the different spin components simultaneously, we physically separate them by briefly applying a strong magnetic field gradient [24] which is perpendicular to the beam symmetry axis, and parallel to gravity. After an additional 20 ms of free-fall and separation, absorption imaging down the axis of symmetry shows the different spin components displaced from each other, giving a picture of the composite spin state of the BEC after interacting with the laser pulses.

In Fig. 3 the results of coherent population transfer for various configurations of the optical fields are shown. Figure 3(a) shows a typical image of the BEC when no optical pulses have been applied. Adjacent to it, Fig. 3(b) is an image taken after performing coherent transfer to $|0\rangle$ using Gaussian beams, which carry no OAM. Note that the transfer efficiency is essentially 100%. This indicates, as expected, that nonlinear interaction terms proportional to the mean-field energy [10–15] are negligible for our present experimental configuration. Figure 3(c) shows results when the Stokes and pump beams are *both* in the LG_0^1 mode. No OAM is transferred ($\Delta l=0$), but a ring-shaped portion of the BEC is transferred to $|0\rangle$, leaving 15% of the atoms in the $|2\rangle$ state in the center.

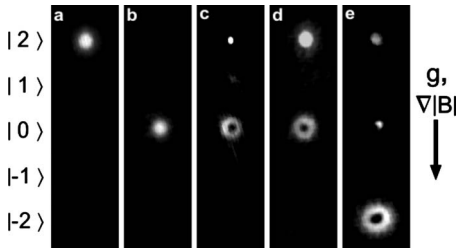

FIG. 3. Axial images of the BEC after spin-state separation. (a) No optical fields applied. (b) Coherent transfer $|2\rangle \rightarrow |0\rangle$ with Gaussian (G) beam modes. (c) $|2\rangle \rightarrow |0\rangle$ with Stokes (pump) beams in LG_0^{-1} (LG_0^{-1}) modes, respectively. For (d) and (e) the beams are detuned −500 MHz from $|1'\rangle$. (d) $|2\rangle \rightarrow |0\rangle$ using Stokes (pump) modes G (LG_0^{-1}). (e) Sequential coupling: $|2\rangle \rightarrow |0\rangle$ using G (LG_0^{-1}) modes, then $|0\rangle \rightarrow |-2\rangle$ using G (LG_0^{1}). The direction of gravity and the B-field gradient is indicated. In the absence of the field gradient, the spin components physically overlap. The field of view of each image is 0.5×2 mm.

In Figs. 3(d), 3(e), and 4, optical beam modes with differing OAM have been used (G and $LG_0^{\pm 1}$), which results in a change of $\mp\hbar$ in the external angular momentum ($\Delta l = \mp 1$). The beams have been detuned −500 MHz from the transition to $|1'\rangle$ to allow use of multiple pulse sequences where only a fraction of the BEC is transferred by each pulse pair. Figure 3(d) shows the results of a single pulse pair transferring 20% of the BEC to the $|0\rangle$ internal state and $l=1$ vortex state. Figure 3(e) shows sequential two-photon coupling, first from $|2\rangle$ to $|0\rangle$, then from $|0\rangle$ to $|-2\rangle$, with a mode configuration that results in $l=0$ for the $|-2\rangle$ state. For confirmation that this was a coherent two-step process, the LG modes for the $|2\rangle \rightarrow |0\rangle$ and the subsequent $|0\rangle \rightarrow |-2\rangle$ transfer stages were slightly displaced from each other, resulting in the small remnant population in $|0\rangle$ observed in the figure.

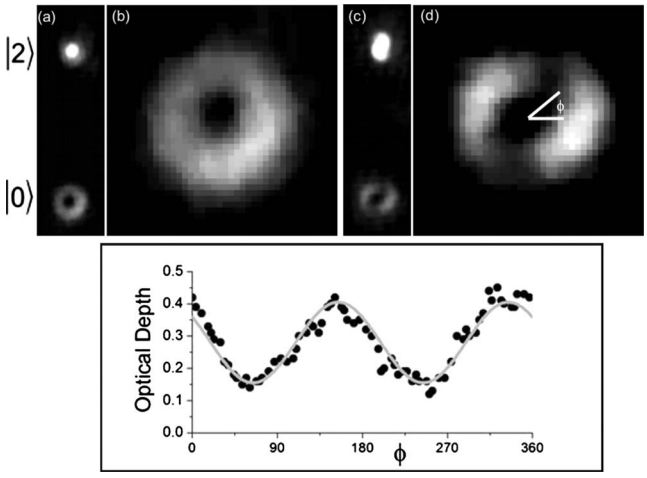

FIG. 4. Coherent superposition of $l=1$ and $l=-1$ vortex states with resulting interference pattern. (a) and (b) Two successive transfers of part of the BEC to the $|0\rangle$, $l=1$ vortex state [using G (LG_0^{-1}) Stokes (pump) beam modes]. (c) and (d) Transfer to the $|0\rangle$, $l=1$ vortex state, followed by transfer to the $|0\rangle$, $l=-1$ state [G (LG_0^{-1}) modes, then G (LG_0^{1})]. The graph is a circular lineout from (d), with a $\sin^2(\phi-\phi_0)$ fit to the data. The field of view in (b) and (d) is 280×280 μm.

The spin textures evident in Figs. 3(c)–3(e) illustrate the potential for generating interesting topological states of the internal spin independently of, or in addition to, the creation of vortex states with external angular momentum. For example, coreless vortices of either Mermin-Ho or Anderson-Toulouse type [25–27] can be created with appropriately designed pulse and mode configurations.

The presence or absence of external angular momentum cannot be inferred from the BEC expansion rate in our experiment. In our present configuration, the additional tangential velocity of atoms in a $l=\pm 1$ vortex state should be $v_\perp = l\hbar/rm_{\mathrm{Rb}} \approx 20$ μm/s. This is an unmeasurable fractional change in the BEC's radial expansion velocity (≈3 mm/s). Note that the $|0\rangle$ components in Figs. 3(c) and 3(d), for which $l=0$ and 1, respectively, are qualitatively indistinguishable from each other. The cloud size differences observed are mainly due to weak configuration-dependent dipole forces from the radial intensity gradient of the LG optical beam modes.

To confirm the presence of quantized vortices in the BEC, we use a procedure that creates a coherent superposition of different vortex states and then observe the resulting interference pattern. Figure 4 shows the results for two cases where 20% of the BEC is coherently transferred from $|2\rangle$ to $|0\rangle$ twice successively, with ($\Delta l = \pm 1$) each time. In Figs. 4(a) and 4(b), part of the BEC has been transferred twice to the $l=1$ vortex state, and no interference is seen. In Figures 4(a) and 4(b), a nearly equal fraction of the BEC has been placed into both the $l=1$ and $l=-1$ states, and an interference pattern is readily apparent. Because the phase of the order parameter for the $l=\pm 1$ vortex states varies as $e^{\pm i\phi}$, where ϕ is the azimuthal angle, their coherent superposition exhibits a $\sin^2(\phi-\phi_0)$ azimuthal amplitude modulation, which is illustrated in the graph in the lower part of the figure. The angle of the azimuthal node depends on the relative phase between the vortex states, which is determined by the optical fields. This interference pattern in the BEC order parameter is analogous to the creation of an optical Hermite-Gaussian beam mode by interference of two opposite-handed Laguerre-Gaussian beam modes.

Generation of coherent superposition states in this manner is not a trivial procedure, in some cases requiring careful consideration of spatially inhomogeneous evolution of the dynamic and geometric phase resulting from the spatially varying intensities of the pump and Stokes laser beam modes [28]. We anticipate that this characteristic of multipulse, multimode coherent population transfer will be an interesting subject for future study.

In summary, we have demonstrated controlled exchange of internal and external angular momentum from optical fields to a BEC and have shown several examples of the spin textures and vortex states in which the BEC can be placed, including coherent superpositions of states of different vorticity. The dynamics of this interaction are complex, with a number of potential topics for further study, including many-body effects [10,16], geometric phase of mesoscopic spins [29], and spin orbit coupling [30].

We expect that these techniques can be readily adapted to work with an optically trapped BEC by accounting for the

trapping potential and mean-field energy in the design of the transfer pulse sequence. Creation of complex spinor BEC states in a trap would be a useful tool for studying the dynamics and stability of such systems (e.g., [31,32]). With improved magnetic field control, this technique could be used in the magnetically degenerate regime, allowing the implementation of proposals for studying ultracold atomic clouds in non-Abelian gauge potentials [33]. Furthermore, it is likely that this system could be used to perform storage and retrieval of OAM states of light [14], which when combined with the ability to manipulate the atomic states may make a so-called vortex phase qubit a viable model system for studies related to quantum computation [15].

The authors thank M. Morris of RPC Photonics Inc. for providing the spiral phase plate used in this work, A. Kowalik and M. Pack for experimental contributions, M. Takahashi for insightful discussions of spin textures, and A. Hansen for helping motivate this avenue of inquiry. This work was supported by the NSF and ARO.

[1] A. E. Ruark and H. C. Urey, Proc. Natl. Acad. Sci. U.S.A. **13**, 763 (1927).
[2] R. A. Beth, Phys. Rev. **50**, 115 (1936).
[3] L. Allen, M. W. Beijersbergen, R. J. C. Spreeuw, and J. P. Woerdman, Phys. Rev. A **45**, 8185 (1992).
[4] J. W. R. Tabosa and D. V. Petrov, Phys. Rev. Lett. **83**, 4967 (1999).
[5] J. Leach, M. J. Padgett, S. M. Barnett, S. Franke-Arnold, and J. Courtial, Phys. Rev. Lett. **88**, 257901 (2002).
[6] R. Feynman, Prog. Low Temp. Phys. **1**, 17 (1955).
[7] G. W. Rayfield and F. Reif, Phys. Rev. Lett. **11**, 305 (1963).
[8] M. R. Matthews, B. P. Anderson, P. C. Haljan, D. S. Hall, C. E. Wieman, and E. A. Cornell, Phys. Rev. Lett. **83**, 2498 (1999).
[9] J. R. Anglin and W. Ketterle, Nature (London) **416**, 211 (2002).
[10] K. P. Marzlin, W. Zhang, and E. M. Wright, Phys. Rev. Lett. **79**, 4728 (1997).
[11] E. L. Bolda and D. F. Walls, Phys. Lett. A **246**, 32 (1998).
[12] R. Dum, J. I. Cirac, M. Lewenstein, and P. Zoller, Phys. Rev. Lett. **80**, 2972 (1998).
[13] G. Nandi, R. Walser, and W. P. Schleich, Phys. Rev. A **69**, 063606 (2004).
[14] Z. Dutton and J. Ruostekoski, Phys. Rev. Lett. **93**, 193602 (2004).
[15] K. T. Kapale and J. P. Dowling, Phys. Rev. Lett. **95**, 173601 (2005).
[16] R. Kanamoto, E. M. Wright, and P. Meystre, Phys. Rev. A **75**, 063623 (2007).
[17] M. F. Andersen, C. Ryu, P. Clade, V. Natarajan, A. Vaziri, K. Helmerson, and W. D. Phillips, Phys. Rev. Lett. **97**, 170406 (2006).
[18] J. E. Williams and M. J. Holland, Nature (London) **401**, 568 (1999).
[19] K. W. Madison, F. Chevy, W. Wohlleben, and J. Dalibard, Phys. Rev. Lett. **84**, 806 (2000).
[20] P. C. Haljan, I. Coddington, P. Engels, and E. A. Cornell, Phys. Rev. Lett. **87**, 210403 (2001).
[21] G. Andrelczyk, M. Brewczyk, L. Dobrek, M. Gajda, and M. Lewenstein, Phys. Rev. A **64**, 043601 (2001).
[22] A. E. Leanhardt, A. Görlitz, A. P. Chikkatur, D. Kielpinski, Y. Shin, D. E. Pritchard, and W. Ketterle, Phys. Rev. Lett. **89**, 190403 (2002).
[23] J. Martin, B. W. Shore, and K. Bergmann, Phys. Rev. A **54**, 1556 (1996).
[24] A. E. Leanhardt, Y. Shin, D. Kielpinski, D. E. Pritchard, and W. Ketterle, Phys. Rev. Lett. **90**, 140403 (2003).
[25] N. D. Mermin and T.-L. Ho, Phys. Rev. Lett. **36**, 594 (1976).
[26] P. W. Anderson and G. Toulouse, Phys. Rev. Lett. **38**, 508 (1977).
[27] T. Mizushima, K. Machida, and T. Kita, Phys. Rev. Lett. **89**, 030401 (2002).
[28] H. Y. Ling, S. Yi, H. Pu, D. E. Grochowski, and W. Zhang, Phys. Rev. A **73**, 053612 (2006).
[29] I. Fuentes-Guridi, J. Pachos, S. Bose, V. Vedral, and S. Choi, Phys. Rev. A **66**, 022102 (2002).
[30] L. Allen, V. E. Lembessis, and M. Babiker, Phys. Rev. A **53**, R2937 (1996).
[31] M. Cozzini, B. Jackson, and S. Stringari, Phys. Rev. A **73**, 013603 (2006).
[32] V. Pietilä, M. Möttönen, and S. M. M. Virtanen, Phys. Rev. A **76**, 023610 (2007).
[33] J. Ruseckas, G. Juzeliunas, P. Ohberg, and M. Fleischhauer, Phys. Rev. Lett. **95**, 010404 (2005).